



HAL
open science

Formation of glassy skins in drying polymer solutions: approximate analytical solutions

Laurence Talini, François Lequeux

► **To cite this version:**

Laurence Talini, François Lequeux. Formation of glassy skins in drying polymer solutions: approximate analytical solutions. *Soft Matter*, 2023, 19 (30), pp.5835-5845. 10.1039/D3SM00522D . hal-04237200

HAL Id: hal-04237200

<https://hal.science/hal-04237200v1>

Submitted on 11 Oct 2023

HAL is a multi-disciplinary open access archive for the deposit and dissemination of scientific research documents, whether they are published or not. The documents may come from teaching and research institutions in France or abroad, or from public or private research centers.

L'archive ouverte pluridisciplinaire **HAL**, est destinée au dépôt et à la diffusion de documents scientifiques de niveau recherche, publiés ou non, émanant des établissements d'enseignement et de recherche français ou étrangers, des laboratoires publics ou privés.

Cite this: DOI: 00.0000/xxxxxxxxxx

Formation of glassy skins in drying polymer solutions: Approximate analytical solutions †

Laurence Talini,^{*a} and François Lequeux^b

Received Date

Accepted Date

DOI: 00.0000/xxxxxxxxxx

We study the formation of a glassy skin at the air interface of drying polymer solutions. We introduce a simple approximation, which is valid for most diffusion problems, and which allows us to derive analytical relationships for the polymer concentration as a function of time. We show that the approximate results differ by less than 15% from those obtained by numerically solving the diffusion equation. We use the approximation to study skin formation in evaporating solutions. We focus on the influence of variations of the mutual diffusion coefficient with concentration, when the latter decreases sharply at high concentrations, as observed in the vicinity of the glass transition. We show that the skin thickness depends very strongly on the exponent characterising the decrease of the diffusion coefficient, in contrast to the polymer volume fraction at the interface, which varies only slightly with the exponent.

1 Introduction

When solvent or suspending fluid is evaporated from a solution or a suspension, a concentration gradient of the respectively dissolved or dispersed phase may build up from the interface with air. This is the case if diffusion does not efficiently scatter the solute that is advected by the flow of solvent toward the interface. A measurement of this effect is given by the Péclet number that compares a characteristic diffusion with a characteristic drying time, $Pe = t_{diffusion}/t_{drying}$. At large Péclet numbers, the interface gets richer in solute as drying proceeds, which may result in the formation of a solid crust or skin. Skin formation is currently observed with large molecules or suspended particles, that have relatively small diffusion coefficients and for which large Péclet numbers can be reached even in conditions of spontaneous solvent evaporation. For instance, it is frequently reported in polymer solutions^{1–7} and colloidal suspensions^{2,8,9}. Nevertheless, a skin can also form when the solute is constituted of smaller objects such as surfactants, provided the drying velocity is large¹⁰. The consequences of crust formation can be dramatic since the crust encloses a still liquid suspension or solution, which volume decreases because of ongoing evaporation whereas the skin surface area remains constant. As a result, the skin may wrinkle⁵, buckle^{1,9,11} or fracture and delaminate^{7,12}. In addition, the skin

may also modify the drying kinetics, as occurs if the mutual diffusion of solvent and solute is concentration-dependent¹³. For instance, the diffusion coefficients of amorphous polymers and their solvents strongly vary with concentration. As a polymer solution gets more concentrated, its coefficient first slightly increases because of the elastic contribution of the polymer network and further decreases by several orders of magnitude in the vicinity of the glass transition in solvent content^{14,15}. This dramatic slowing down of diffusion is combined with the non linear decrease of the activity of solvent as the solvent content vanishes¹⁶. In addition, hysteretic effects in the relationship between solvent activity and concentration in solution lead to further complexity of the drying behaviour^{17,18}. As a result, the full drying of films of polymer solutions can require times up to several weeks.

It is thus crucial in applications to determine whether a skin builds up in order to predict the drying time, or adapt the drying conditions to prevent the formation of defects of the dried film. Even if the skin can be so thin that it requires specially designed experiments to be evidenced^{3,5,7,19}, its presence may have a significant impact on the dry deposit. Using a scaling law analysis, de Gennes²⁰ showed that a skin of thickness smaller than 100nm could form at the interface of a drying polymer solution and, by its subsequent rupture, induce large surface roughness of dried polymer films. More recently, a model based on the analysis of asymptotic behaviours demonstrated that the onset of skin formation can be inferred from the variations of film thickness as a function of time¹³. The latter model allows a description of the different stages involved in the drying of a polymer solution, and gives the conditions for skin formation when the diffu-

^a CNRS, Surface du Verre et Interfaces, Saint-Gobain, Aubervilliers, France. E-mail: laurence.talini@cnrs.fr

^b CNRS Sciences et Ingénierie de la Matière Molle, ESPCI Paris, PSL Research University, Sorbonne Université, Paris, France.

† Electronic Supplementary Information (ESI) available: [details of any supplementary information available should be included here]. See DOI: 00.0000/00000000.

sion coefficient linearly increases with concentration. However, it does not provide quantitative information on the concentration gradient and skin thickness as drying proceeds, for which a full resolution of the diffusion equation is required. Actually, fully analytical approaches are made difficult by the complexity of the diffusion equation; in addition to the non-linearity resulting from the concentration dependence of the diffusion coefficient, a moving boundary condition is involved since the interface with air is displaced during drying. As a result, the problem is generally solved numerically^{21–25}. In the last decade, it was shown that a solute Lagrangian scheme could simplify the problem^{26,27}. In this frame, the problem reduces to a diffusion equation that accounts for the moving boundary condition. The latter equation - that involves a concentration-dependent diffusion coefficient - could be solved numerically and new insight was provided on skin formation. However, as in other works¹³, only a linear increase with concentration of the mutual diffusion coefficient of solvent and polymer was considered, which captures what happens at intermediate polymer concentrations when a gel phase is formed, but not the behaviour close to glass transition. The large variations and singularities of the diffusion coefficient associated with glass transition are indeed difficult to handle numerically.

Here, we focus on the effect of the vicinity of glass transitions on drying of polymer solutions. We use a similar Lagrangian scheme as the one already suggested²⁷ in order to establish a diffusion equation, which is verified by an effective concentration. In addition, we introduce an approximation that allows a straightforward resolution of any diffusion equation provided its associated boundary conditions varies slowly with time. We use the latter approximation to derive analytical expressions of the skin thickness and surface concentration. The approximated results, that are shown to be very close to numerical findings, are further used to examine the effects of large variations and possible singularity of the diffusion coefficient with concentration.

The paper is organised as follows: in section 2, we show how the problem can be reduced to a diffusion problem with a non constant diffusion coefficient by considering the relative amount of solvent in the drying solution instead of a volume fraction. In section 3, we provide a very simple approximation of the solution to a diffusion equation, and show for pedagogical purposes how it can be used in diffusion problems with a constant diffusion coefficient, and with a boundary condition of either a constant concentration or a constant flux. In section 4, we extend the approximation to situations in which the diffusion coefficient may vary by several orders of magnitude as drying proceeds. Finally in section 5, we solve the commonly encountered case of solvent evaporation from a polymer solution.

2 Diffusion equations

We consider a unidimensional problem. As schematised in figure 1, the polymer solution is located at $z > 0$, and evaporation occurs at its interface with air, which is initially at $z = 0$. We consider a non confined solution and we assume that, far from the interface, in the limit where $z \rightarrow \infty$, the solvent volume fraction is not affected by evaporation. Therefore, during drying, the interface as well as the solute are displaced toward the positive values of z .

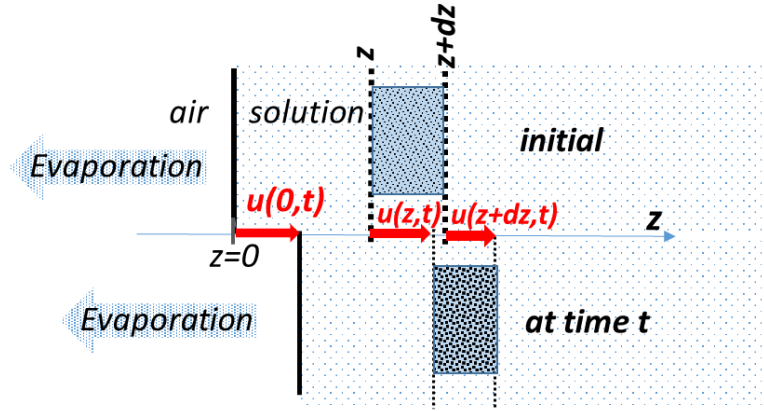


Fig. 1 Scheme of the considered drying geometry. The solution is initially in the region $z > 0$. Solvent evaporation results in a displacement of the solute $u(z,t)$. At time t , the layer initially located between z and $z+dz$ is between $z+u(z,t)$ and $z+dz+u(z+dz,t)$.

We denote as $u(z,t)$ the displacement - with respect to the laboratory frame - of the solute at position z at time $t = 0$. For the sake of simplicity, we assume volume additivity of solvent and solute. The initial volume fraction of solute is uniform and denoted ϕ_0 . We consider the volume of solute $\phi_0 dz$ located between z and $z+dz$ at time $t = 0$. At time t , it has moved between $z+u(z,t)$ and $z+dz+u(z+dz,t) = z+u(z,t) + (1+u_z(z,t))dz$ where $u_z(z,t)$ is the derivative of u with respect to z . Note that both $u(z)$ and $u_z(z)$ go to zero for $z \rightarrow \infty$. Therefore, the volume fraction of solute at position $z' = z+u(z,t)$ and at time t is

$$\phi(z',t) = \frac{\phi_0}{1+u_z} \quad (1)$$

In the frame of the laboratory, the flux of solute j and solvent j_{liq} oppose at any given position z' and are given by Fick's law

$$j(z') = -j_{liq}(z') = -D_{mut} \frac{\partial \phi}{\partial z'} \quad (2)$$

where D_{mut} is the mutual diffusion coefficient of the solvent and polymer which depends on ϕ . The flux of solute at position z' is

$$j(z') = \phi \frac{\partial u(z)}{\partial t} \quad (3)$$

The transport equation is obtained by combining equations 2 and 3

$$\frac{\partial u(z)}{\partial t} = -\frac{D_{mut}}{\phi(z')} \frac{\partial \phi}{\partial z'} \quad (4)$$

which can be written using equation 1 and the relation $dz' = (1+u_z)dz$

$$\frac{\partial u}{\partial t} = \frac{D_{mut}}{(1+u_z)^2} \frac{\partial u_z}{\partial z} \quad (5)$$

in which we have omitted the variable z for the sake of simplicity as now all variables depend on z only. Further derivating equation 5 with respect to z yields

$$\frac{\partial u_z}{\partial t} = \frac{\partial}{\partial z} \left(\frac{D_{mut}}{(1+u_z)^2} \frac{\partial u_z}{\partial z} \right) \quad (6)$$

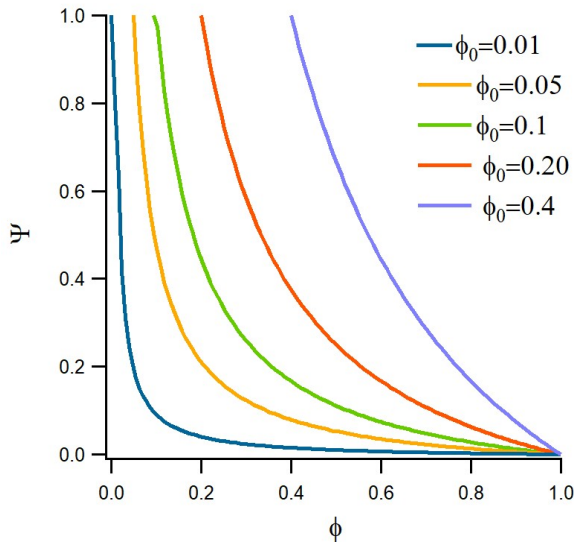


Fig. 2 Normalised solvent uptake Ψ as a function of solute volume fraction ϕ for various initial values ϕ_0 of solute volume fraction.

The latter equation is a non-linear diffusion equation. As already demonstrated²⁷, the moving boundary condition - intrinsic to drying problem - can be circumvented by changing the variable of interest. In order to solve equation 6, we introduce a more convenient variable corresponding to the relative amount of solvent in the system, which we denote as Ψ and define as

$$\Psi = 1 + \frac{u_z}{1 - \phi_0} \quad (7)$$

At time $t = 0$, $\Psi = 1$ and when solvent has fully evaporated, $\Psi = 0$. $1 - \Psi(z)$ corresponds to the fraction of solvent evaporated from a slice of solution located at position z . In particular, the total volume of solvent evaporated from the solution and normalised by the initial volume fraction of solvent is obtained by integration of $1 - \Psi$, i.e.

$$\int_0^\infty (1 - \Psi) dz = \frac{u(0, t)}{1 - \phi_0} \quad (8)$$

Using equation 1, Ψ can also be expressed as a function of ϕ , which yields

$$\Psi = \frac{\phi_0}{(1 - \phi_0)} \frac{(1 - \phi)}{\phi} \quad (9)$$

The variations of Ψ as a function of ϕ are shown in figure 2 for different initial volume fractions in solute. For a given value of ϕ , Ψ increases with increasing initial volume fraction ϕ_0 since a dilute solution shrinks more than a concentrated one during drying.

Equation 6 that is verified by Ψ can be written as

$$\frac{\partial \Psi}{\partial t} = \frac{\partial}{\partial z} \left(D(\Psi) \frac{\partial \Psi}{\partial z} \right) \quad (10)$$

where the apparent diffusion coefficient is given by

$$D(\Psi) = \frac{D_{mut}(\phi)}{(\Psi(1 - \phi_0) + \phi_0)^2} \quad (11)$$

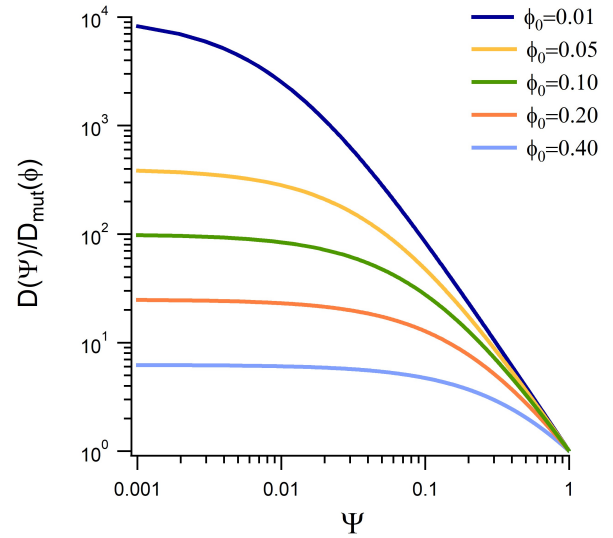


Fig. 3 Ratio of the apparent and mutual diffusion coefficients as a function of Ψ for different initial values ϕ_0 of solute volume fraction.

The variations with volume fraction of the ratio of the apparent and mutual diffusion coefficients are shown in figure 3. The less concentrated in solute the initial solution, the larger the contraction of the solution during drying, which is accounted for by larger values of $D(\Psi)/D_{mut}(\phi)$ for small initial volume fractions.

We now examine the boundary condition that is associated with equation 10. Integrating the latter equation with respect to z and using equation 8 yields

$$\left(D(\Psi) \frac{\partial \Psi}{\partial z} \right)_{z=0} - J_{ev} = 0 \quad (12)$$

where J_{ev} is the positive quantity of solvent evaporated from the solution per time unit and normalised by the initial volume fraction of solvent. J_{ev} is expressed as an evaporation velocity and is given by

$$J_{ev} = \frac{1}{1 - \phi_0} \frac{\partial u(0, t)}{\partial t} \quad (13)$$

In summary, we have shown that the moving boundary condition involved during drying can be accounted for by a non-linear diffusion equation with a fixed boundary condition. A Lagrangian description is thus used, as suggested in previous works^{26,27}. Here, we introduce a convenient variable, Ψ , which is the relative amount of solvent with respect to the initial one, and the equation verified by Ψ is written with respect to the initial space variable, z . The associated diffusion coefficient is given by the mutual diffusion coefficient of polymer and solvent, and a Ψ -dependent term that accounts for the contraction of the solution during drying. Actually, the diffusion coefficient increases as the solution dries because the latter shrinks as solvent evaporates.

Hence, the problem is strictly equivalent to diffusion with a concentration-dependent diffusion coefficient. This problem has been addressed in the past²⁸, but an analytical solution can be found only for a constant concentration at the boundary. In the following section, we show how equations having the general form of equation 10 can be solved analytically by mean of an

approximation.

For pedagogical purposes, we first introduce the approximation in simple situations and compare its predictions to exact resolutions. We further use it in a more general case.

3 Approximation for the resolution of diffusion equations with constant diffusion coefficients

First, we introduce an approximation to solve linear diffusion equations, i.e. for a constant diffusion coefficient D . Consideration of this simple situation allows a comparison of the approximate solutions to the exact ones, since the latter can be obtained analytically. The approximation is valid for slowly varying concentration fields, which is in general observed since the diffusion equation involves a second derivative with respect to the space coordinate. As a result, the fluctuation mode of wave vector q has a damping rate given by Dq^2 , which quickly increases with decreasing wavelength. Therefore, fluctuation modes of large wavelengths are favored and smooth concentration fields are expected; in addition, if the boundary conditions, or any other control parameters, evolve slowly compared to the spontaneous evolution under diffusion, they do not introduce short length disturbance. For these reasons, small wavelength effects can generally be neglected in diffusion problems. Hence, we suggest a *long wavelength* approximation that consists in replacing the solution $\Psi(z, t)$ by an approximate concentration $\Psi^{ap}(z, t)$ varying linearly in space. Actually, in the non confined solution we consider, Ψ is expected to increase from a finite value at $z = 0$ to reach $\Psi = 1$ for $z \rightarrow \infty$. Therefore, we suggest the following approximation for Ψ

$$\Psi^{ap} = \frac{1 - \Psi_s}{\xi(t)} z + \Psi_s(t) \quad (14)$$

for $0 < z < \xi(t)$ and $\Psi^{ap} = 1$ for $z > \xi(t)$. $\Psi_s(t)$ and $\xi(t)$ are two time-dependent parameters that are respectively the value of Ψ at $z = 0$ and the characteristic length over which Ψ varies. In the following, we consider two different boundary conditions at $z = 0$ and we examine the approximate and exact solutions to equation 10.

3.1 Exact and approximate solution for a constant value at the boundary

We assume that $\Psi = 1$ in the whole solution at time $t = 0$ and that Ψ further takes a constant value at $z = 0$, i.e. $\Psi(0, t) = \Psi_s$. The situation is equivalent to the classical problem of heat diffusion in a semi-infinite medium with an initially homogeneous temperature, and an imposed constant temperature at the boundary. Its exact solution is

$$\Psi(z, t) = \Psi_s + (1 - \Psi_s) \operatorname{erf}\left(\frac{z}{2\sqrt{Dt}}\right) \quad (15)$$

We now approximate Ψ by equation 14. Since Ψ_s is held constant, the only time dependent parameter is $\xi(t)$. A flux - analogous to a heat flux in the heat problem - can be associated with Ψ : it is given by $D(1 - \Psi_s)/\xi(t)$. The region in which Ψ has diffused at time t (corresponding to the region in which the temperature has changed in the heat problem) has a surface area

$(1 - \Psi_s)\xi(t)/2$. The time derivative of the latter must be equal to the flux, yielding

$$\frac{D(1 - \Psi_s)}{\xi(t)} = \frac{\partial}{\partial t} \left(\frac{\xi(t)(1 - \Psi_s)}{2} \right) \quad (16)$$

the solution to which is $\xi(t) = 2\sqrt{Dt}$, which is the same characteristic diffusion length as the one in equation 15. Both approximate and exact solutions, respectively given by equations 14 and 15, are shown in figure 4. Their variations are very close to one another in the vicinity of the interface with air at which the value of Ψ is given. The discrepancy exhibited close to the bottom interface (with the region non affected by drying) results from a poor prediction of the flux in the frame of the approximation. However, space and time variations remain close and the approximate flux at the interface, given by $0.5(1 - \Psi_s)\sqrt{\frac{D}{t}}$, is only about 10% smaller than the exact one, $J(0, t) \simeq 0.56(1 - \Psi_s)\sqrt{\frac{D}{t}}$.

3.2 Exact and approximate solution for a constant flux at the boundary

We now apply the above approximation to solve the diffusion equation with a constant flux J_{ev} at $z = 0$ imposed at $t = 0$. The problem is then analogous to a heat problem with an imposed constant heat flux. We use the same linear expression Ψ^{ap} as in the former subsection but with Ψ_s and ξ both depending on time. The condition of constant flux is

$$J_{ev} = \frac{D(1 - \Psi_s(t))}{\xi(t)} \quad (17)$$

The same balance as in equation 16 can be used with a time dependent value of Ψ_s , which yields after integration with respect to time

$$J_{ev}t = \frac{\xi(t)(1 - \Psi_s(t))}{2} \quad (18)$$

Combining equations 17 and 18, we obtain $\Psi_s(t) = 1 - J_{ev}\sqrt{\frac{2t}{D}}$ and $\xi(t) = \sqrt{2Dt}$. The exact solution to equation 10 with a constant flux at $z = 0$ is²⁸

$$\Psi(z, t) = 1 + \frac{J_{ev}}{D} \left[z \left(1 - \operatorname{erf}\left(\frac{z}{2\sqrt{Dt}}\right) \right) - 2\sqrt{\frac{Dt}{\pi}} e^{-\frac{z^2}{4Dt}} \right] \quad (19)$$

Both exact and approximate solutions are shown in figure 4. Since the value of the flux is given, the slope is well predicted but discrepancies are observed for the values of Ψ close to the interfaces.

The value of Ψ_s inferred from equation 19 is

$$\Psi_s(t) = 1 - J_{ev} \frac{2}{\sqrt{\pi}} \sqrt{\frac{t}{D}} \quad (20)$$

whereas the approximate one is

$$\Psi_s^{ap}(t) = 1 - J_{ev} \sqrt{2} \sqrt{\frac{t}{D}} \quad (21)$$

The expressions for Ψ_s only differ by a numerical factor, and Ψ_s is underestimated by about 25% in the approximation.

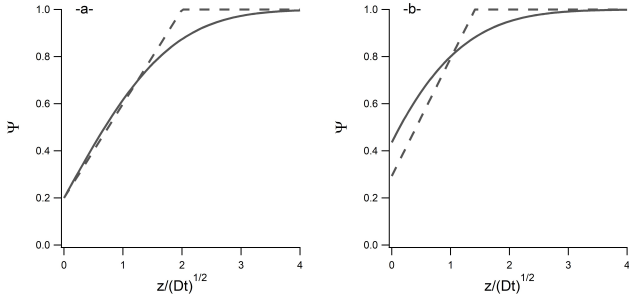


Fig. 4 Exact (full line) and approximated (dashed line) solutions of the linear diffusion equation for a boundary condition at $z=0$ of constant Ψ (a) and constant flux (b). The values of the parameters are $\Psi_s = 0.2$ in (a) and $t = \frac{1}{4}$, $D = 1$ and $J_{ev} = 1$ in (b).

In summary, we have introduced an approximation to solve diffusion equations with constant diffusion coefficients. We have shown that it provides simple analytical expressions and predicts the same variation laws with the different parameters as the exact solutions. Now that the basis of the approximation is laid, we demonstrate in the following how it can be used in the case of interest herein, i.e. a diffusion equation with a non-constant diffusion coefficient.

4 Extension of the approximation to concentration-dependent diffusion coefficients

The approximation we have introduced above consists in assuming a linear variation of Ψ with z , i.e. a space-independent value of $D \frac{\partial \Psi}{\partial z}$ over the diffusion length ξ . We have shown that solutions based on the latter assumption provide a good approximation of the profiles with constant diffusion coefficients. In the following, we make the same approximation with concentration-dependent diffusion coefficients, i.e. that the flux given by

$$J = D(\Psi) \frac{\partial \Psi}{\partial z} \quad (22)$$

is constant between $z=0$ and $z=\xi$, and that $\Psi=1$ for $z>\xi$. The same assumption was made by de Gennes²⁰. As detailed below, if D vanishes as in the vicinity of glass transition, the concentration gradient becomes very large, consistently with the formation of thin glassy skins at the free surface of solution or gels that are observed in experiments⁵.

In the following, we first justify the assumption of a constant flux in a case in which analytical expressions can be found.

4.1 Justification of the constant-flux approximation in the diffusion layer

The aim of this subsection is to compute the flux within the diffusion length ξ and show that it is sensible to approximate it as a constant. For the sake of clarity, we consider a boundary condition of constant $\Psi = \Psi_s$ at the interface, for which an analytical solution to equation 10 can be found. Actually, in this condition, the solution can be written under the form $\Psi = g(\hat{z})$ where $\hat{z} = z/\sqrt{D_0 t}$ and $D_0 = D(\Psi=1)$ ²⁸. We further introduce the function f

$$f(\Psi) = D(\Psi)/D_0 \quad (23)$$

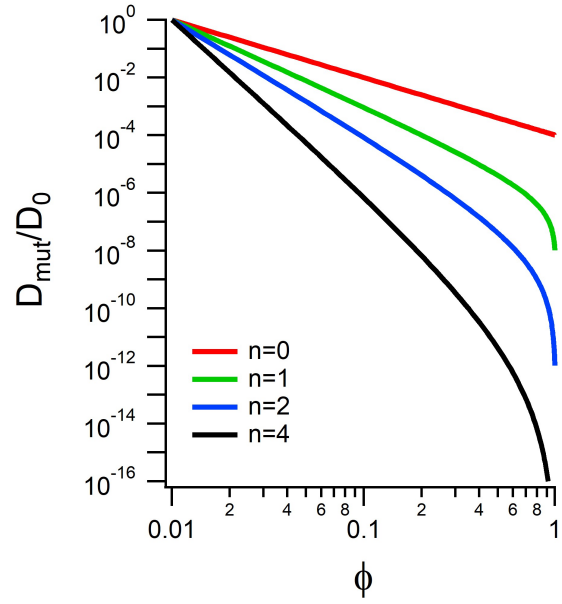


Fig. 5 Ratio of the mutual diffusion coefficient D_{mut} and D_0 as a function of solute volume fraction corresponding to power law variations of $D(\Psi)$ according to equations 11 and 25, for different values of the exponent n .

Equation 10 then leads to

$$g'(\hat{z})^2 f'(g(\hat{z})) + f(g(\hat{z})) g''(\hat{z}) + \frac{1}{2} \hat{z} g'(\hat{z}) = 0 \quad (24)$$

and the boundary conditions correspond to $g(0) = \Psi_s$ and $g(+\infty) = 1$. Since we want to investigate the effect of a singular diffusion coefficient resulting e.g. from glass transition, we adopt the following form for function f

$$f = \Psi^n \quad (25)$$

where n is a positive exponent. Such a power law variation of $D(\Psi)$ corresponds to a mutual diffusion coefficient that follows $D_{mut} \propto (1-\phi)^n/\phi^{n+2}$, i.e. strongly decreasing as the solution dries, similarly to amorphous polymers and their solvents close to their glass transition¹⁵. The variations of D_{mut} are shown in figure 5 for values of the exponent ranging from $n=0$ to $n=4$ for which the decrease is increasingly steeper. In contrast to other works in the literature^{23,25}, the increase of the mutual diffusion coefficient with volume fraction reported in polymer solutions well below the glass transition in solvent content is not reproduced by the chosen variation law. However, the increase remains moderate compared to the decrease close to glass transition¹⁵, and it is expected to have a small effect on skin formation. We emphasise that it could easily be taken into account with the approximation we introduce but would lead to more complex expressions. The simple power law we consider has therefore the advantage of being easily tractable and allows one to capture the physical trends.

With the chosen form of function f , equation 24 becomes

$$g(\hat{z})^n g''(\hat{z}) + n g(\hat{z})^{n-1} g'(\hat{z})^2 + \frac{1}{2} \hat{z} g'(\hat{z}) = 0 \quad (26)$$

We assume that $\Psi_s \rightarrow 0$, expansion of equation 26 near $\hat{z}=0$ then

yields

$$g(\hat{z}) = A\hat{z}^{\frac{1}{n+1}} + 0\left(\hat{z}^{\frac{n+2}{n+1}}\right) \quad (27)$$

where A depends on n and is of order one. The flux is readily obtained from equation 27

$$J = \frac{A^{n+1}}{(n+1)} \sqrt{\frac{D_0}{t}} + 0(z) \quad (28)$$

We emphasise that the flux given by equation 28 exhibits no singularity and does not depend on z at the leading order, whatever the variations of the diffusion coefficient. The approximation of a constant flux within the diffusion length ξ is therefore fully justified. As already assumed in²⁰, we will therefore consider that the flux is constant at any time in the region affected by drying (where $\Psi < 1$). Obviously, this approximation is valid provided the evaporation rate varies more slowly than the spontaneous evolution of the concentration profile in the solution. In the next subsection, we give the relations obtained in the frame of the constant flux approximation, which are valid whatever the boundary condition at the interface.

4.2 Approximate solution to the diffusion equation in the general case:

Except in the specific case discussed above, there is no exact analytical solution to equation 10. In particular, the reduced variable \hat{z} is not compatible with a boundary condition of fixed flux at the interface. We show in what follows that the approximation we have introduced nonetheless provides an analytical expression of the solution in that case. As explained above, we assume a constant flux $J = J_{ev}$ for $0 < z < \xi$, whereas $\Psi(z) = 1$ for $z \geq \xi$.

The expression for ξ is obtained by integration over z of equation 22 between $\Psi_s(t)$ and 1, where $\Psi_s(t)$ is the time-dependent concentration at the interface. Using equation 23, it yields

$$\xi(t) = \frac{D_0}{J_{ev}} \int_{\Psi_s(t)}^1 f(w)dw \quad (29)$$

Equation 29 is equivalent to equation 17 in the non-linear case. Similarly, the Ψ profile is given by integration of equation 22 between $z = 0$ and z , yielding an implicit relation verified by the approximate solution $\Psi(z, t)$. Therefore, between $z = 0$ and $z = \xi$, the approximate solution follows

$$z = \xi \frac{\int_{\Psi_s(t)}^{\Psi(z,t)} f(w)dw}{\int_{\Psi_s(t)}^1 f(w)dw} \quad (30)$$

and by $\Psi = 1$ for $z > \xi$. In order to close the problem, the time evolution of Ψ_s must be derived. As established in section 2, the total volume of evaporated solvent per surface unit is given by the integral of $1 - \Psi$ between $z = 0$ to $z = \xi$. Changing the integration variable using $dz = \frac{d\xi}{d\Psi} d\Psi$ together with equation 22 yields the following expression of the evaporated volume

$$\int_0^\xi (1 - \Psi(z, t)) dz = \xi(t) \frac{\int_{\Psi_s(t)}^1 (1 - w) f(w) dw}{\int_{\Psi_s(t)}^1 f(w) dw} \quad (31)$$

Lastly, the derivative with respect to time of the evaporated

volume must be equal to the drying velocity, yielding the relation

$$J_{ev} = \frac{d}{dt} \left[\int_0^\xi (1 - \Psi(z, t)) dz \right] \quad (32)$$

Equations 29 and 32 allow the determination of both Ψ_s and ξ as a function of time during drying. In the case of a constant diffusion coefficient (corresponding to $f = 1$), equations 17 and 18 established in section 3 are recovered.

In the next section, we focus on realistic conditions of evaporation of a polymer solution, and we show how the spatial variations of the polymer volume fraction can be approximated in these conditions.

5 Evaporation conditions

We assume now that the solvent evaporates and that its vapour diffuses over a boundary layer of thickness Λ above which the concentration of vapour is zero. We denote D_{gas} the diffusion coefficient of the vapour in the atmosphere. With the notation adopted above, the evaporation velocity is $\frac{\partial w}{\partial t}$. It depends on the activity of the solvent, $\gamma(1 - \phi_s)$ where γ is the activity coefficient of the solvent, equal to 1 for an ideal solution and ϕ_s the polymer volume fraction at the interface. Since the concentration in solvent vapor is the saturation concentration c_{sat} at the interface with the solution and zero at a distance Λ , the evaporation velocity is $D_{gas} c_{sat} \gamma(1 - \phi_s(t)) / \Lambda \rho$ with ρ is the density of solvent in the liquid state. The velocity J_{ev} defined in equation 13 is then given by

$$J_{ev} = \frac{D_{gas} c_{sat} \gamma}{\Lambda \rho} \frac{1 - \phi_s(t)}{1 - \phi_0} \quad (33)$$

We consider a constant activity coefficient which does not reproduce the non-linearity of the sorption isotherm of polymers¹⁶⁻¹⁸ but nonetheless captures the decrease of the evaporation flux as the solution dries²⁰. In addition, it has the advantage of providing simpler analytical relations. Our results could nevertheless be extended to more complex variations of the solvent activity.

In the limit $\phi_s \rightarrow 1$, equation 33 yields

$$J_{ev} \simeq \frac{D_{gas} c_{sat} \gamma \Psi_s}{\Lambda \rho \phi_0} \quad (34)$$

The evaporation kinetics is determined by equations 29 and 32. A characteristic length λ and characteristic time τ can be defined respectively as

$$\lambda = \frac{D_0 \Lambda \rho \phi_0}{D_{gas} c_{sat} \gamma} \quad (35)$$

and

$$\tau = D_0 \left(\frac{\Lambda \rho \phi_0}{D_{gas} c_{sat} \gamma} \right)^2 \quad (36)$$

For numerical values that are typical of evaporating aqueous solutions, $D_0 = 10^{-10} \text{ m}^2 \cdot \text{s}^{-1}$, $D_{gas} = 10^{-5} \text{ m}^2 \cdot \text{s}^{-1}$, $c_{sat} = 10^{-2} \text{ kg} \cdot \text{m}^{-3}$, $\rho = 10^3 \text{ kg} \cdot \text{m}^{-3}$, $\Lambda = 5 \text{ mm}$. With, in addition, $\phi_0 = 0.1$ and $\gamma = 0.5$, the length and time scales are $\lambda \simeq 1 \text{ mm}$ and $\tau \simeq 10^4 \text{ s}$. In the following, we determine the variations with time of the value of Ψ at the interface.

5.1 Time variations of surface concentration

The relation between ξ and Ψ_s is given by equation 29, which becomes

$$\xi(t) = \frac{\lambda}{\Psi_s(t)} \int_{\Psi_s}^1 f(w)dw \quad (37)$$

and the time evolution of Ψ_s is given by equation 32 that writes now

$$\Psi_s(t) = \tau \frac{d}{dt} \left(\frac{1}{\Psi_s} \int_{\Psi_s}^1 (1-w)f(w)dw \right) \quad (38)$$

The latter equation is an implicit equation, which for $\Psi_s \rightarrow 0$, yields at the leading order in Ψ_s

$$\frac{d\Psi_s}{\Psi_s^3} \left(\int_0^1 (1-w)f(w)dw + O(\Psi_s) \right) = -\frac{dt}{\tau} \quad (39)$$

The solutions to respectively equation 38 and equation 10 are shown in figure 6. The solution to equation 10 was obtained by numerical resolution following the procedure detailed in the Supplemental Information. The variations with time of of both the exact and approximated surface volume fraction ϕ_s are displayed in the same figure. They were inferred from the obtained values of Ψ_s using equation 9 and for $\phi_0 = 0.1$. For both Ψ_s and ϕ_s , solutions to the simple differential equation 38 successfully approximate the exact solutions since they underestimate them by less than 15%. At the maximal chosen time $t = 100\tau$, the solution is not dry. Its volume fraction at the interface remains smaller than unity, in agreement with the very long drying times. Interestingly, the asymptotic behaviours of Ψ_s and ϕ_s only weakly depend on the behaviour of the diffusion coefficient $D(\Psi)$ - i.e. on $f(\Psi)$ - close to $\Psi = 0$. For instance, at the final chose time $t = 100\tau$, ϕ_s is larger by less than 20% for $n = 4$ corresponding to a large singularity of D_{mut} than for $n = 0$ for which D_{mut} more smoothly decreases with increasing volume fractions (see figure 5). Actually, the dependence of D with Ψ is accounted for in the integrals of $f(\Psi)$ and respectively $(1-\Psi)f(\Psi)$ in the numerator of equations 37 and 38, which do not exhibit any singularity when $\Psi_s \rightarrow 0$. The only singular term is the Ψ_s^{-1} term in the r.h.s. of equations 37 and 38, and results from the vanishing drying velocity when the surface of the solution is nearly completely dry. Obviously, from equation 37, the same weak dependence on the value of the exponent n is expected for ξ .

When $t \rightarrow \infty$, the asymptotic behavior of Ψ_s , can be deduced from equation 38 and is

$$\Psi_s(t) \simeq \left(1 + \frac{t}{\bar{\tau}} \right)^{-\frac{1}{2}} \quad (40)$$

where $\bar{\tau} = \tau \int_0^1 f(w)(1-w)dw$. The asymptotic limits are shown for two values of the exponent n in figure 6. They slightly overestimate Ψ_s . We will use equation 40 to determine the thickness of the skin that forms at the interface. Moreover, the total thickness of the layer depleted in solvent can be deduced from equations 40 and 37 in the limit $t \gg \tau$

$$\xi(t) = \lambda \frac{t^{1/2}}{\tau^{1/2}} \frac{\int_0^1 f(w)dw}{\int_0^1 f(w)(1-w)dw} \quad (41)$$

Therefore, the simple result $\xi \propto \sqrt{D_0 t}$ is obtained. The prefactor,

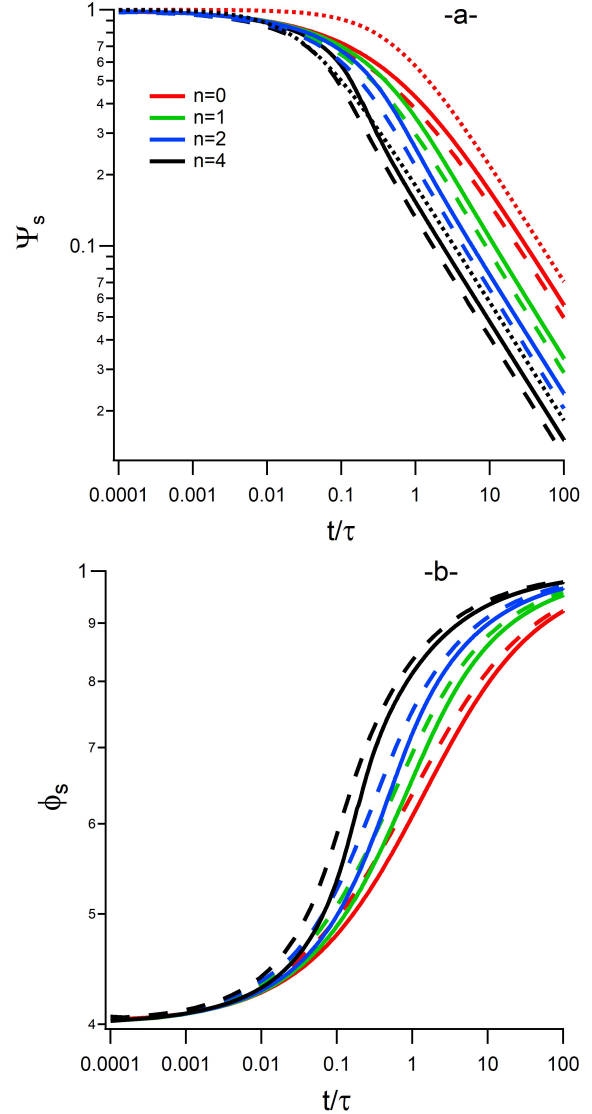


Fig. 6 (a) Surface value of Ψ , Ψ_s , and (b) corresponding surface volume fraction ϕ_s as functions of the reduced time for different values of the exponent n in evaporation conditions. Full integration of equation 10 (full lines) is shown together with the approximated solutions given by equation 38 (dashed lines). In (a), the asymptotic limits given by equation 40 are shown for $n = 0$ and $n = 4$ (dotted lines). In (b), the initial volume fraction is $\phi_0 = 0.4$.

which is the ratio of the two integrals of f in the r.h.s. of equation 41, is of order one. We emphasise that the Peclet number defined with length ξ , $Pe_\xi = \frac{D_0}{J_{ev}\xi} \simeq 1$ is of order unity. We will see in section 5.3 that a different analysis can be made in terms of Peclet number for the onset of skin formation.

In the following subsection, we show that, in contrast to what is observed for the values at the interface, the spatial profiles are significantly affected by the behaviour of $D(\Psi)$.

5.2 Spatial profiles

First, we establish an approximate expression of the spatial variations of Ψ . Combining equations 29 and 37 yields

$$z = \frac{\lambda}{\Psi_s} \int_{\Psi_s}^{\Psi} f(w) dw \quad (42)$$

We recall that z is the spatial coordinate of the solution in its initial state.

Using a function f that has a form given by equation 25, equation 42 becomes

$$z(\Psi) = \lambda \frac{\Psi^{n+1} - \Psi_s^{n+1}}{(n+1)\Psi_s} \quad (43)$$

The corresponding spatial variations of Ψ are shown in figure 7 where the value of Ψ_s is the one at $t/\tau = 100$ obtained by numerical integration of equation 38. The profiles are very close to the ones obtained from numerical resolution of equation 10, which once again confirms the efficiency of the approximation.

The variations of the volume fraction in solute in the drying solution, i.e. $\phi(z')$ can be inferred from the $\Psi(z)$ profiles established above. We recall that the spatial coordinate in the drying solution is $z' = z + u(z)$. We denote z'_s the position of the interface. We define h as the distance to the interface during drying. Thus $h(z) = z + u(z) - u(0) = z' - z'_s$. Notations are indicated in figure 8

The depth in the drying solution at which a given value Ψ is found, i.e. $h(\Psi) = z' - z'_s$, is found by integration of u_z

$$h(\Psi) = z(\Psi) + \int_0^{z(\Psi)} u_z(x) dx = \int_0^{z(\Psi)} (\Psi(x)(1 - \phi_0) + \phi_0) dx \quad (44)$$

After change of variables following equation 42, the depth can be written as

$$h(\Psi) = \lambda \int_{\Psi_s}^{\Psi} (w(1 - \phi_0) + \phi_0) \frac{f(w)}{\Psi_s} dw \quad (45)$$

Using the definition of Ψ given by equation 9, it is possible to compute respectively the exact and approximated volume fractions as a function of the distance to the interface given by equation 45. Their variations are shown in figure 7b. The exact and approximated solutions for ϕ are very close. They significantly depend on the variations of the diffusion coefficient. As already reported above, the value of ϕ at the interface moderately increases with n . In contrast, the value of ϕ at large enough distance from the interface (for instance at $z = \lambda$) decreases with increasing values of n and, for $n = 4$, it is almost half the value for $n = 0$. The smaller concentrations for large n result from the smaller average value of the diffusion coefficient.

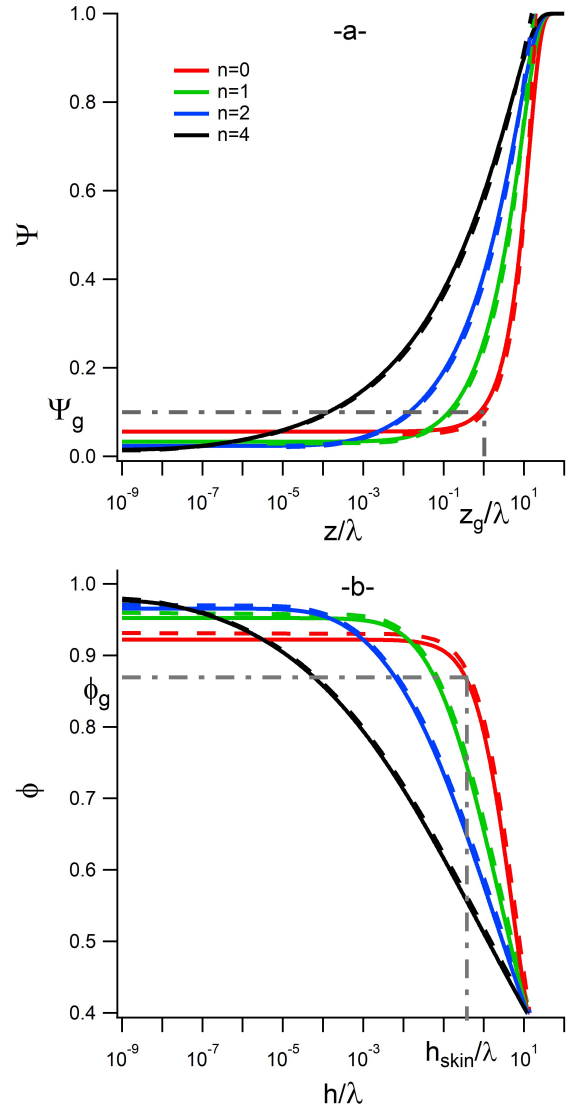


Fig. 7 (a) Ψ and (b) corresponding volume fraction ϕ as functions of the normalised distance from the interface, respectively with respect to the initial coordinate z in (a) and to the distance to the interface in the drying solution, h in (b). The values have been computed at time $t = 100\tau$ in the evaporation conditions we consider and for an initial volume fraction $\phi_0 = 0.4$. Integration of equation 10 (full lines) is shown together with the approximate solutions (dashed lines) given by equation 43 after numerical integration of equation 38. The curves in (b) are inferred from the ones in (a) using respectively equation 9 and 45. The dashed-dotted lines respectively indicate the arbitrarily chosen value of $\Psi_g = 0.1$ in (a) and the corresponding value of $\phi_g = 0.87$ in (b) that have been used to compute the skin thickness, as well as the corresponding values of z_g/λ and h_{skin}/λ for $n = 0$.

5.3 Skin thickness

The thickness of the skin that forms at the interface can be computed in the frame of the hypotheses made above. We arbitrarily define the thickness z_g as the distance at which Ψ reaches the value $\Psi_g = 0.1$. As indicated in figure 7, it corresponds to a volume fraction $\phi_g = 0.56$. The skin thickness $z_g = z(\Psi_g)$ has been computed using either the complete numerical resolution of the problem, or equation 43, in which the values of $\Psi_s(t)$ were deduced from integration of equation 38. The skin thickness with respect to the drying solution, h_{skin} , is obtained by integration of equation 45, yielding

$$h_{skin} = \frac{\lambda}{\Psi_s} \left(\frac{\Psi_g^{n+2} - \Psi_s^{n+2}}{n+2} (1 - \phi_0) + \frac{\Psi_g^{n+1} - \Psi_s^{n+1}}{n+1} \phi_0 \right) \quad (46)$$

Figure 9 displays the variation with the normalised time of both the thickness with respect to the initial solution and the real thickness h_{skin} . The approximation underestimates the formation time t_{skin} by about 20% but, at later times, the approximated thickness is very close to the exact one.

Noticeably, the skin forms at a finite time and both its thickness and apparition time depend on the variations with concentration of the diffusion coefficient. More precisely, the sharper the decrease of the diffusion coefficient, the earlier the apparition of the skin and the smaller its thickness. The time at which skin formation occurs rather weakly depends on exponent n since it decreases by one order of magnitude as the exponent n increases from 0 to 4. In contrast, the thickness value varies by about four orders of magnitude in the same exponent range. With the typical numerical values we have given in what precedes, the initial value of the skin thickness ranges from a few nanometers for $n = 4$ to a few hundreds of microns for $n = 0$. Consistently, glassy crusts of very different thicknesses have been evidenced experimentally^{5,7}.

The time t_{skin} at which the skin appears is simply given by the equation $\Psi_s(t_{skin}) = \Psi_g$, that yields, using equation 40 and assuming that $\Psi_g^2 \ll 1$

$$t_{skin} \simeq \frac{\bar{\tau}}{\Psi_g^2} \quad (47)$$

An estimate of the skin thickness just after its formation is obtained from equation 46 by considering that $\Psi_s = \Psi_g/2$. It can be approximated as

$$h_{skin}(t_{skin}) \simeq 2\lambda\Psi_g^n \left(\frac{(1 - \phi_0)\Psi_g}{n+2} + \frac{\phi_0}{n+1} \right) \quad (48)$$

The skin thickness when it forms therefore verifies $h_{skin} \propto \frac{D(\Psi_g)}{J_w}$. The same scaling law was established by de Gennes²⁰, even though he adopted a different definition of skin thickness that yielded a dependency on volume fraction different from the one of equation 48.

In the present analysis, in addition to its value when it forms, the time variations of skin thickness can also be examined. Using equation 43, for large time when $\Psi_s \simeq \sqrt{\bar{\tau}/t}$, the skin thickness

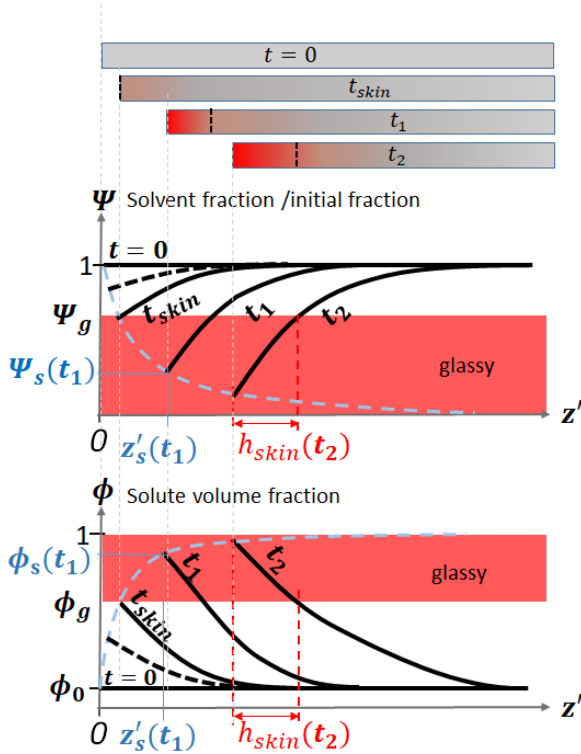


Fig. 8 Scheme of the drying sample in the laboratory frame and schematic variations of the ratio of solvent fraction and its initial value, Ψ and of the polymer volume fraction, ϕ . During drying, the solution shrinks, the position of the solute in the laboratory frame is denoted z' , and the solute volume fraction at the surface Φ_s increases with time. It reaches a value above Φ_g at time t_{skin} . Hence, a glassy layer appears and further expands with time. Its thickness is denoted h_{skin} .

has the following asymptotic limit

$$h_{skin} = \lambda \left(\frac{\Psi_g^{n+2}}{n+2} (1 - \phi_0) + \frac{\Psi_g^{n+1}}{n+1} \phi_0 \right) \sqrt{\frac{t}{\tau}} \quad (49)$$

The predicted behaviour $h_{skin} \propto t^{1/2}$, which, remarkably, does not depend on n , is observed in figure 9. The skin growth velocity therefore decreases with time. Even if a skin forms earlier when the diffusion coefficient strongly decreases in the vicinity of glass transition, it can nonetheless remain very thin. Therefore, it may have less dramatic consequences on the final state of the dry layer than the thicker skin formed at later times for more moderate decreases of the diffusion coefficient with concentration.

In the literature, a criterion on the Péclet number has been suggested to determine the formation of a skin^{26,29}. However, it was established for gel phases in which the diffusion coefficient linearly increases with polymer concentration. Actually, the scaling law we have found for h_{skin} does correspond to a Péclet number defined with the value of the mutual diffusion coefficient in the skin, yielding $Pe_{skin} = \frac{D(\Psi_g)}{J_{ev} h_{skin}} \simeq 1$. Finally, we emphasise that, even if the diffusion coefficient in the skin is vanishingly small, the evaporation is never limited by solvent diffusion through the skin. Actually, the solvent activity at the surface of the solution decreases with increasing polymer volume fraction. Therefore, the formation of a glassy skin is associated with a decrease of the evaporation flux and this decrease governs the drying kinetics. Hence, it is necessary to consider a non constant evaporation flux in order to fully account for the behaviours of drying polymer solutions.

6 Conclusions

In conclusion, in this work we describe a way to establish approximate analytical solutions to non-linear diffusion equations. The method combines a Lagrangian description with an approximation based on simple considerations of matter conservation. We apply it to the drying of amorphous polymer solutions and we investigate the formation of a crust at the interface with air during drying when the mutual diffusion coefficient strongly decreases with increasing polymer concentration, as observed near the glass transition. We show that the difference between the approximated and concentration profiles is less than 15%. Our analytical results provide new insight on the skin formation when glass transition is at stake. In particular, we show that i) the time at which the skin appears only weakly depends on the precise variations of the mutual diffusion coefficient with volume fraction, ii) in contrast when it forms, the skin has a thickness that varies by several orders of magnitude according to the variations of the diffusion coefficient, and may be very small (nanometric), iii) after its formation, the skin thickness always increases with the square root of time. The concentration gradient varies as the inverse of the mutual diffusion coefficient and, can be so large that the skin thickness goes down to molecular sizes.

Author Contributions

The two authors contributed equally to the work.

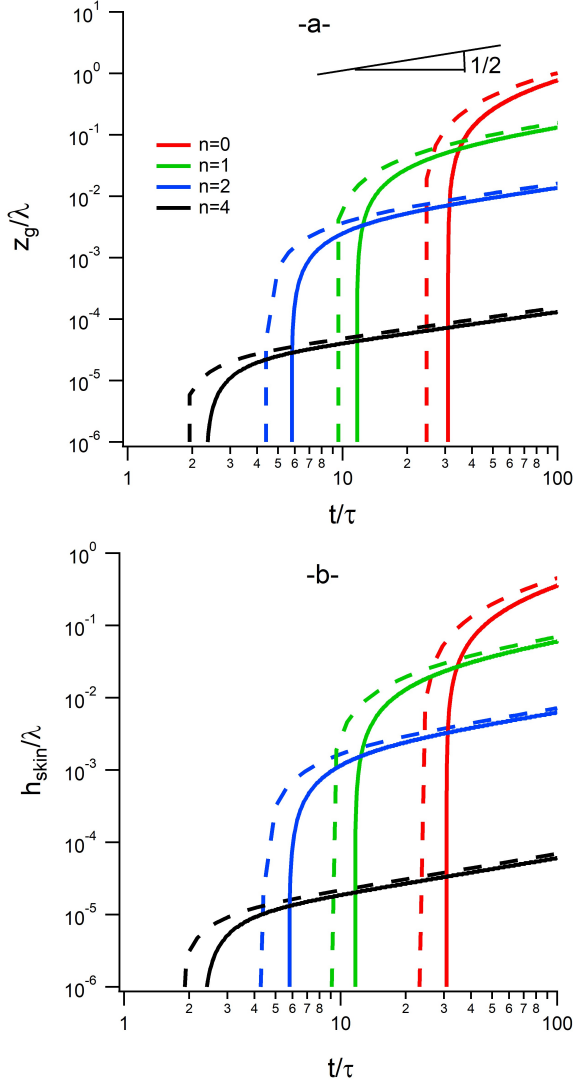


Fig. 9 (a) Thickness of the skin z_g normalised by the characteristic length λ and as a function of the normalised time t/τ in the considered evaporation conditions. z_g is arbitrarily defined as the distance at which $\Psi = \Psi_g = 0.1$ with respect to the initial solution, and is obtained both by integration of equation 10 (full lines) and using the approximate solution (dashed lines) given by equations 37 and 38. (b) Corresponding skin thickness in the drying solution as a function of time given by the approximated expression of equation 45 with $\phi_0 = 0.4$.

Conflicts of interest

There are no conflicts to declare.

Notes and references

- 1 Pauchard L, Allain C. Buckling instability induced by polymer solution drying. *Europhys Lett.* 2003 Jun;62(6):897-903. Available from: <https://iopscience.iop.org/article/10.1209/epl/i2003-00457-7>.
- 2 Ekanayake P, McDonald PJ, Keddie JL. An experimental test of the scaling prediction for the spatial distribution of water during the drying of colloidal films. *Eur Phys J Spec Top.* 2009 Jan;166(1):21-7. Available from: <http://link.springer.com/10.1140/epjst/e2009-00872-4>.
- 3 Shimokawa Y, Kajiya T, Sakai K, Doi M. Measurement of the skin layer in the drying process of a polymer solution. *Phys Rev E.* 2011 Nov;84(5):051803. Available from: <https://link.aps.org/doi/10.1103/PhysRevE.84.051803>.
- 4 Arai S, Doi M. Skin formation and bubble growth during drying process of polymer solution. *Eur Phys J E.* 2012 Jul;35(7):57. Available from: <http://link.springer.com/10.1140/epje/i2012-12057-2>.
- 5 Huraux K, Narita T, Bresson B, Frétiigny C, Lequeux F. Wrinkling of a nanometric glassy skin/crust induced by drying in poly(vinyl alcohol) gels. *Soft Matter.* 2012;8(31):8075. Available from: <http://xlink.rsc.org/?DOI=c2sm25480h>.
- 6 Arya RK, Tewari K, Shukla S. Non-Fickian drying of binary polymeric coatings: Depth profiling study using confocal Raman spectroscopy. *Progress in Organic Coatings.* 2016 Jun;95:8-19. Available from: <https://linkinghub.elsevier.com/retrieve/pii/S0300944015302617>.
- 7 Tirumkudulu MS, Punati VS. Solventborne Polymer Coatings: Drying, Film Formation, Stress Evolution, and Failure. *Langmuir.* 2022 Mar;38(8):2409-14. Available from: <https://pubs.acs.org/doi/10.1021/acs.langmuir.1c03124>.
- 8 Style RW, Peppin SSL. Crust formation in drying colloidal suspensions. *Proceedings of the Royal Society A: Mathematical, Physical and Engineering Sciences.* 2010 Jun;467(2125):174-93. Publisher: Royal Society. Available from: <https://royalsocietypublishing.org/doi/full/10.1098/rspa.2010.0039>.
- 9 Boulogne F, Giorgiutti-Dauphine F, Pauchard L. The buckling and invagination process during consolidation of colloidal droplets. *Soft Matter.* 2013;9(3):750-7. Place: Cambridge Publisher: Royal Soc Chemistry WOS:000312335500015. Available from: <https://www.webofscience.com/wos/woscc/full-record/WOS:000312335500015>.
- 10 Moreau F, Colinet P, Dorbolo S. Explosive Leidenfrost droplets. *Phys Rev Fluids.* 2019 Jan;4(1):013602. Available from: <https://link.aps.org/doi/10.1103/PhysRevFluids.4.013602>.
- 11 Lintingre Ducouret G, Lequeux F, Olanier L, Périé T, Talini L. Controlling the buckling instability of drying droplets of suspensions through colloidal interactions. *Soft Matter.* 2015;11(18):3660-5. Available from: <http://xlink.rsc.org/?DOI=C5SM00283D>.
- 12 Tomar BS, Shahin A, Tirumkudulu MS. Cracking in drying films of polymer solutions. *Soft Matter.* 2020;16(14):3476-84. Available from: <http://xlink.rsc.org/?DOI=C9SM02294E>.
- 13 Hennessy MG, Ferretti GL, Cabral JT, Matar OK. A minimal model for solvent evaporation and absorption in thin films. *Journal of Colloid and Interface Science.* 2017 Feb;488:61-71. Available from: <https://linkinghub.elsevier.com/retrieve/pii/S0021979716308402>.
- 14 Neogi P. *Diffusion in Polymers.* CRC Press; 1996. Google-Books-ID: j9XcvXNDwtQC.
- 15 Rauch J, Köhler W. *Diffusion and Thermal Diffusion of Semidilute to Concentrated Solutions of Polystyrene in Toluene in the Vicinity of the Glass Transition.* *Phys Rev Lett.* 2002 Apr;88(18):185901. Available from: <https://link.aps.org/doi/10.1103/PhysRevLett.88.185901>.
- 16 Saby-Dubreuil AC, Guerrier B, Allain C, Johannsmann D. Glass transition induced by solvent desorption for statistical MMA/ n BMA copolymers — Influence of copolymer composition. *Polymer.* 2001 Feb;42(4):1383-91. Available from: <https://linkinghub.elsevier.com/retrieve/pii/S0032386100005395>.
- 17 Leibler L, Sekimoto K. On the sorption of gases and liquids in glassy polymers. *Macromolecules.* 1993 Dec;26(25):6937-9. Available from: <https://pubs.acs.org/doi/abs/10.1021/ma00077a034>.
- 18 Richardson H, Sferrazza M, Keddie JL. Influence of the glass transition on solvent loss from spin-cast glassy polymer thin films. *Eur Phys J E.* 2003 Nov;12(S1):87-91. Available from: <http://link.springer.com/10.1140/epjed/e2003-01-021-5>.
- 19 Kajiya T, Sawai D, Miyata K, Miyashita Y, Noda H. Simple method to measure rheological properties of soft surfaces by a micro-needle contact. *Eur Phys J E.* 2022 Sep;45(9):76. Available from: <https://link.springer.com/10.1140/epje/s10189-022-00227-w>.
- 20 de Gennes PG. Solvent evaporation of spin cast films: “crust” effects. *Eur Phys J E.* 2002 Jan;7(1):31-4. Available from: <http://link.springer.com/10.1140/epje/i200101169>.
- 21 Bornside DE, Macosko CW, Scriven LE. Spin coating: One-dimensional model. *Journal of Applied Physics.* 1989 Dec;66(11):5185-93. Publisher: American Institute of Physics. Available from: <https://aip.scitation.org/doi/10.1063/1.343754>.
- 22 Wong SS, Altinkaya SA, Mallapragada SK. Understanding the effect of skin formation on the removal of solvents from semicrystalline polymers. *J Polym Sci B Polym Phys.* 2005 Nov;43(22):3191-204. Available from: <https://onlinelibrary.wiley.com/doi/10.1002/polb.20615>.
- 23 Ozawa K, Okuzono T, Doi M. Diffusion Process during Drying to Cause the Skin Formation in Polymer Solutions. *Jpn J Appl Phys.* 2006 Nov;45(11R):8817. Available from: <https://iopscience.iop.org/article/10.1143/JJAP.45.8817>.
- 24 Hennessy MG, Breward CJW, Please CP. A Two-Phase Model

- for Evaporating Solvent-Polymer Mixtures. *SIAM J Appl Math.* 2016 Jan;76(4):1711-36. Available from: <http://epubs.siam.org/doi/10.1137/15M1035707>.
- 25 Punati VS, Tirumkudulu MS. Modeling the drying of polymer coatings. *Soft Matter.* 2022;18(1):214-27. Available from: <http://xlink.rsc.org/?DOI=D1SM01343B>.
- 26 Luo L, Meng F, Zhang J, Doi M. Skin formation in drying a film of soft matter solutions: Application of solute based Lagrangian scheme. *Chinese Phys B.* 2016 Jul;25(7):076801. Available from: <https://iopscience.iop.org/article/10.1088/1674-1056/25/7/076801>.
- 27 Meng F, Luo L, Doi M, Ouyang Z. Solute based Lagrangian scheme in modeling the drying process of soft matter solutions. *Eur Phys J E.* 2016 Feb;39(2):22. Place: New York Publisher: Springer WOS:000371323200003. Available from: <https://www.webofscience.com/wos/woscc/full-record/WOS:000371323200003>.
- 28 Crank J. *The Mathematics of Diffusion.* Clarendon Press; 1979. Google-Books-ID: eHANhZwVouYC.
- 29 Okuzono T, Ozawa K, Doi M. Simple model of skin formation caused by solvent evaporation in polymer solutions. *Phys Rev Lett.* 2006 Sep;97(13):136103. Place: College Pk Publisher: American Physical Soc WOS:000240872700040. Available from: <https://www.webofscience.com/wos/woscc/full-record/WOS:000240872700040>.